nature human behaviour

ARTICLES

https://doi.org/10.1038/s41562-019-0556-z

Human non-olfactory cognition phase-locked with inhalation

Ofer Perl[1,2*], Aharon Ravia[1,2], Mica Rubinson[3], Ami Eisen[3], Timna Soroka[1,2], Nofar Mor[1,2], Lavi Secundo[1,2] and Noam Sobel[1,2*]

Olfactory stimulus acquisition is perfectly synchronized with inhalation, which tunes neuronal ensembles for incoming information. Because olfaction is an ancient sensory system that provided a template for brain evolution, we hypothesized that this link persisted, and therefore nasal inhalations may also tune the brain for acquisition of non-olfactory information. To test this, we measured nasal airflow and electroencephalography during various non-olfactory cognitive tasks. We observed that participants spontaneously inhale at non-olfactory cognitive task onset and that such inhalations shift brain functional network architecture. Concentrating on visuospatial perception, we observed that nasal inhalation drove increased task-related brain activity in specific task-related brain regions and resulted in improved performance accuracy in the visuospatial task. Thus, mental processes with no link to olfaction are nevertheless phase-locked with nasal inhalation, consistent with the notion of an olfaction-based template in the evolution of human brain function.

Terrestrial mammalian olfaction relies on sniffing for odorant transport[1]. Moreover, sniffs alone, with no odorants, orchestrate neural activity in the olfactory receptors[2], bulb[3–5] and cortex[6,7]. In other words, sniffs prime the rhinencephalon (literally from Greek: the nose-brain or smell-brain) for incoming olfactory information[8,9]. Olfaction is often referred to as an ancient sense[10], reflecting its primacy in human evolution[11]. In this respect, the olfactory system can be thought of as a template for human brain development[12,13]. Given that this brain evolutionary template relies on inspirium for information processing onset, our overarching hypothesis is that the entire human brain retained aspects of this functional link. Consistent with an important role for respiration in human brain function[14], we hypothesize that nasal inhalations, which put the olfactory system in a mode that optimizes processing of incoming information, similarly optimize non-olfactory mechanisms for incoming information as well.

The notion that overall brain activity is linked to overall respiratory cycles is well documented[14,15]. There is extensive evidence in rodents for global[16] and local[17,18] brain rhythms that are entrained by respiration, and evidence for similar effects in humans[19,20]. However, our hypothesis is not about an overall effect of respiratory cycles on brain cycles, but rather a more specific hypothesis on respiratory phase: we predict specific differences in cognitive processing and ensuing behaviour during inhalation versus exhalation. This too, has support in the animal literature. For example, sniffing is linked to both whisking[21,22] and vocalizations[23] in mice, and to wing beating and echolocation[24,25] in bats. In other words, inhalations may orchestrate diverse complex behaviours[26]. In humans, nasal inhalation affects patterns of activity in the primary olfactory cortex as evidenced with functional magnetic resonance imaging (fMRI)[6] and intracranial electroencephalography (iEEG)[27], and impacts cognition that relies on these limbic structures. More specifically, odour imagery is enhanced by nasal inhalations[28], reaction time in discrimination of facial fear is faster during nasal inhalation, as is memory retrieval[27,29,30]. However, these tasks all rely on rhinencephalic amygdaloidal and hippocampal substrates that are also part of the primary olfactory cortex, where sniffing is an inherent modulator of activity. Here, to ask whether this is a general brain property rather than an olfactory substrate property alone, we tested whether nasal inhalation affects performance in cognitive tasks that are less hinging on limbic substrates. We had participants perform visuospatial and lexical tasks, during either nasal inhalation or exhalation, and concurrently measured brain activity using EEG. We found that participants spontaneously opted to inhale at task onset, that performance in the visuospatial task was significantly better during inhalation versus exhalation, and that localized task-related brain activity was greater on inhalation than on exhalation. Moreover, inhalation shifted brain connectivity at rest, and this shift was correlated with ensuing inhalation-dependent improvements in behavioural accuracy. In other words, we could generate modest but significant predictions of respiratory-phase-dependent shifts in performance using previously recorded phase-dependent neural activity. These results support our notion of a general brain information-processing mode triggered by inhalation, and are consistent with our hypothesis of an olfaction-guided aspect in the evolution of human non-olfactory cognition.

Results

Humans spontaneously nasally inhale at cognitive task onset. In experiment 1, we first asked whether participants unwittingly spontaneously opt to perform cognitive tasks at any particular phase of the respiratory cycle. Concurrent with precise measurement of nasal airflow (Fig. 1a), 31 participants (15 women, mean age = 25.67 ± 2.27 years) conducted three tasks in succession: a lexical task, a visuospatial task and a math task (order counterbalanced) (Fig. 1b). The lexical task was a lexical decision paradigm (adapted from ref. [31]) in which participants had to judge whether on-screen words or pseudo-words had semantic meaning (for example, 'lexical' versus 'xlical'). The visuospatial task was a two-alternative selection between two simultaneously presented three-dimensional

[1]Department of Neurobiology, Weizmann Institute of Science, Rehovot, Israel. [2]Azrieli Center for Human Brain Imaging and Research, Weizmann Institute of Science, Rehovot, Israel. [3]Department of Physics of Complex Systems, Weizmann Institute of Science, Rehovot, Israel. *e-mail: oferikoo@gmail.com; noam.sobel@weizmann.ac.il

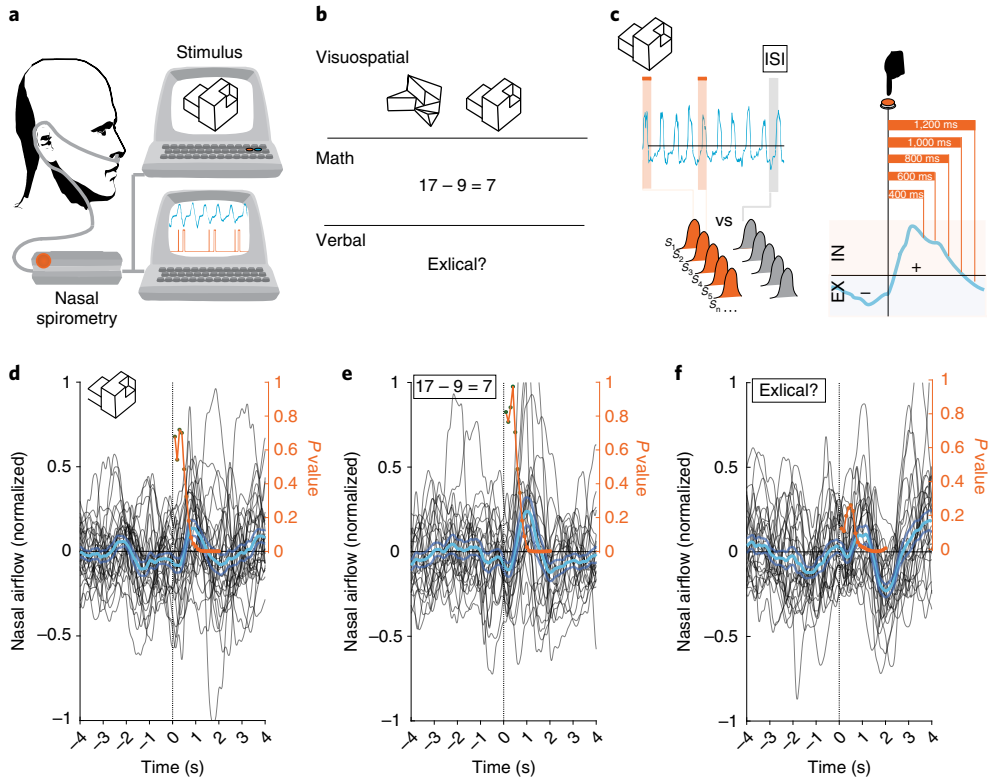

Fig. 1 | Humans spontaneously nasally inhale at cognitive task onset. a, Experimental setup. **b**, Task examples. **c**, Statistical analysis of the respiratory signal. The obtained distribution of real events was compared with surrogate data obtained from random windows of the same size along the respiratory trace. An example respiratory trace is shown in light blue. Trial onset and surrogate time windows are denoted with orange and grey rectangles, respectively. EX, exhale; IN, inhale. **d**–**f**, Mean ± s.e. of the event-related respiratory response of all participants (light blue trace) in the visuospatial ($n = 29$) (**d**), math ($n = 26$) (**e**) and lexical ($n = 24$) (**f**) tasks. Time 0 denotes task initiation (dashed black line). The black traces are individual mean respiration, with inhalation plotted upwards. Overlaid in orange (right *y* axis) is the *P* value obtained per time window tested.

shapes, where only one could exist in the real world, that is, all its facets were correctly joined (adapted from ref. [32]). The math task relied on arithmetic calculations and consisted of equations presented to the participant who had to judge whether they were true or false. Each task contained 25 trials separated by a jittered inter-stimulus-interval (ISI) ranging between 15 and 20 s, culminating at ~10 min per task (Fig. 1c). Finally, in all tasks, participants self-initiated precise trial onset as follows: following the ISI, an on-screen instruction read 'press the button when you are ready for the next trial'. Participants then pressed a button to initiate every trial and a keyboard key to provide answers. Participants were instructed to press the button only when they felt ready to optimally conduct a trial and to then answer as fast and as accurately as possible.

The averaged nasal airflow trace revealed that participants spontaneously opted to initiate trials concurrent with the initiation of a nasal inhalation. Given that participants spent 37.8 ± 6.4% of the time inhaling and 50.7 ± 6.6% exhaling (some participants also had a nasal 'dead-flow' time in between, which amounted for 11.4 ± 6.9% of the time), we calculated the deviation from this expected pattern by comparing to surrogate randomly selected time points (Fig. 1c), and observe that the tendency to nasally inhale at task onset was significant in all tasks (visuospatial: maximal at 1,800 ms post-task onset, trial = 0.52 ± 0.24 normalized flow units (NFU), surrogate = 0.34 ± 0.08 NFU, two-tailed paired *t*-test $t(28) = 3.77$, $P < 0.001$, Cohen's $d = 0.97$, 95% CI = $0.41 \leq d \leq 1.50$; lexical: maximal at 1,600 ms post-task onset, trial = 0.51 ± 0.25 NFU, surrogate = 0.33 ± 0.09 NFU, two-tailed paired *t*-test $t(25) = 3.21$, $P = 0.0035$, Cohen's $d = 0.93$, 95% CI = $0.35 \leq d \leq 1.49$; math: maximal at 1,500 ms post-task onset, trial = 0.54 ± 0.28 NFU, surrogate = 0.31 ± 0.05 NFU, two-tailed paired *t*-test $t(23) = 3.82$, $P < 0.001$, Cohen's $d = 1.14$, 95% CI = $0.52 \leq d \leq 1.74$) (Fig. 1d–f, compare to random surrogate data, and Supplementary Fig. 1a–c). Moreover, a control analysis verified that these nasal inhalations were different from inhalations associated with button press alone (Supplementary Fig. 1d–f). In other words, we observed a significant tendency for participants to time the onset of a non-limbic cognitive effort to coincide with nasal inhalation.

In experiment 2, we asked whether the spontaneous inhalation that we observed at task onset in experiment 1 is related to performance, and if so, how is this reflected in brain activity. In this experiment, we probe for brain-evoked responses, necessitating many more trials per condition. Thus, to accommodate viable total task duration, we discontinued the math task. Thirty participants were then studied first over a 20-min resting baseline, and then when conducting 160-trial versions of the visuospatial and lexical decision tasks, all concurrent with EEG. Here, unbeknownst to participants, half of the trials were triggered by inhalation and half by exhalation (random order). We mislead participants, telling them that trials are randomly triggered over time. Post-experimental debriefing implied that no participant was aware of self-triggering trials. Stimuli were displayed for 1,200 ms, and participants were allowed an additional 300 ms to respond. This assured that each trial was restricted to a given respiratory phase.

Inhalation drives changes in functional brain connectivity at rest. Before analysing behaviour and brain activity during the task, we set out to ask whether there is a pattern of brain activity associated with inhalation versus exhalation at rest. Given that at rest we have

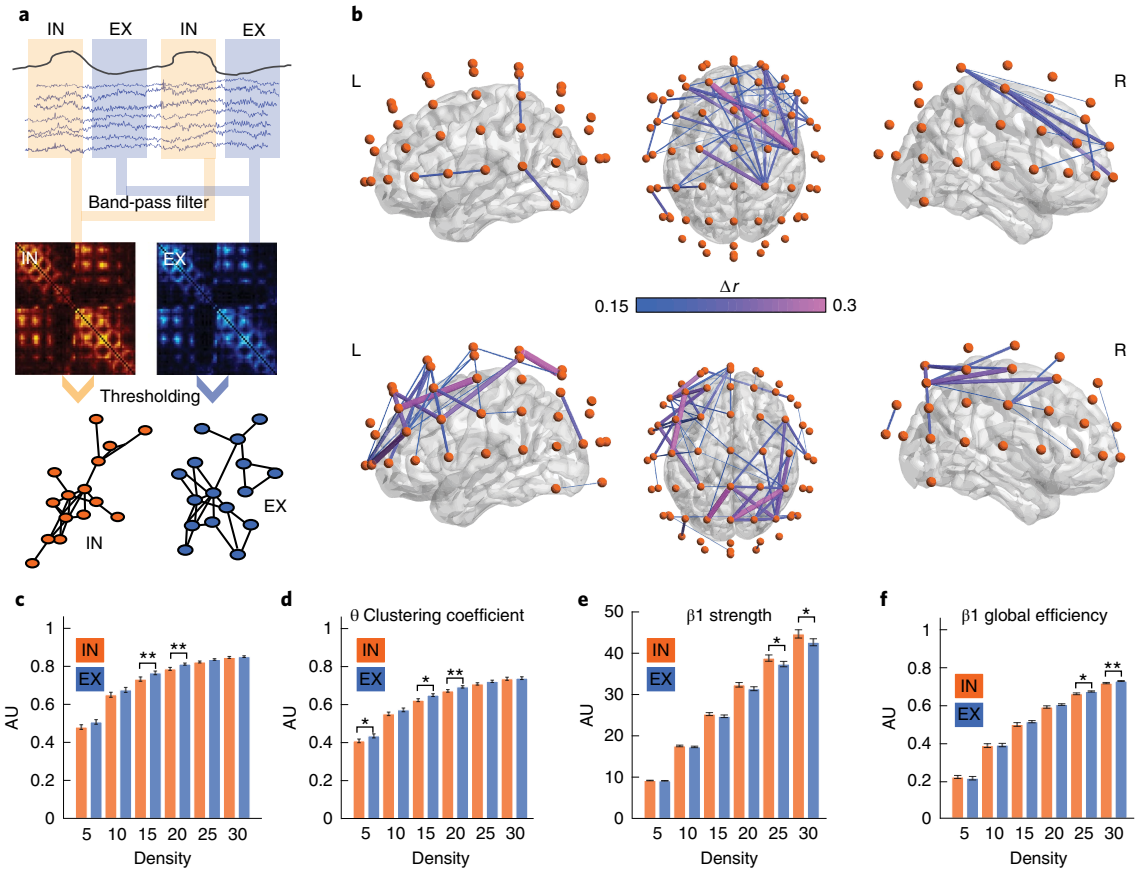

Fig. 2 | Inhalation drives changes in functional brain connectivity at rest. a, Analysis pipeline for graph theory analysis[33]. We extracted EEG epochs occurring exclusively during inhalation and exhalation, which, following band-pass filtering, were used to generate functional connectivity matrices, generated through Pearson correlation. Following thresholding, the remaining edges formed graphs to be analysed using network measurements (see network connectivity analysis in 'Methods'). **b**, Visualization of functional connectivity[62] ($n = 29$): the delta range between connectivity matrices generated from inhale and exhale epochs. The two panels depict connections within the theta frequency band (average density threshold = 15) that were stronger when contrasting inhale > exhale (top panels) and exhale > inhale (bottom panels) across the group. Differential correlation (Δr) between electrodes (orange spheres surrounding the scalp according to 10–20 system coordinates) is represented by lines (width and colour code of Δr value). **c**, Mean ± s.e. of the functional connectivity network local efficiency measurements in the theta frequency band calculated from EEG epochs obtained during nasal inhalation and exhalation ($n = 28$). Measurements were compared in six incremental predefined average density bins (5–30). $^{*}P < 0.05$, $^{**}P < 0.01$. AU, arbitrary units. **d**–**f**, As in **c**, but with different measurements and frequencies as noted ($n = 28$). See Supplementary Table 1 for complete statistical details.

no event-related components, we used graph theory[33] to investigate the effect of respiratory phase on network connectivity during the 20-min baseline recording before task onset. In graph theory, signals acquired from the brain can be represented as a graph—nodes denote different brain areas (in this case, electrode recording sites) and edges represent functional connectivity (Fig. 2a).

The emerging topology of the graphs can be quantified using network measurements, each targeting different aspects of connectivity between neighbouring or distant nodes. We investigated network properties within five discrete frequency bins: delta: 0.5–4 Hz, theta: 4–8 Hz, alpha: 8–12 Hz, beta1: 12–16.5 Hz and beta2: 16.5–24 Hz. Using these data sets, we next constructed graphs as follows: edges were defined using the absolute values of pairwise Pearson correlations applied to all electrode data with no time delay. Next, the correlation matrix was thresholded, and all edges that did not survive were removed, retaining an undirected binary graph (with the exception of the strength measurement, which relied on the weighted version of the graphs). We used six incremental threshold values of average degree (see below) ranging between 5% and 30% as cut-offs (that is, 5% implies that out of 100 nodes, each node is connected on average to five other nodes). We then extracted the following network connectivity measures reiteratively per average density and frequency band[33]: (1) strength: reflecting correlation values of signals recorded from two nodes. (2) Betweenness centrality: reflecting the prevalence of nodes acting as bridges between parts of the network. (3) Global efficiency: reflecting the ability of the network to support long-range transfer of information. (4) Local efficiency: reflecting the resistance of a network structure to 'attack,' that is, incremental disconnections. (5) Clustering coefficient: reflecting the degree of dense interconnectivity between neighbouring nodes (for more details, see 'Network connectivity analysis' in Methods). Finally, to explore the effect of respiratory phase on cortical connectivity, we entered these data into an omnibus analysis of variance (ANOVA) with conditions of phase (inhale and exhale), average density (5, 10, 15, 20, 25 and 30) and measurement (strength, betweenness, mean local efficiency, global efficiency and clustering coefficient). We observed main effects and interactions of measurement and average density, which are trivial given the different units and thresholds used for each calculation. More meaningfully, the ANOVA uncovered a three-way interaction between phase, measurement and average density, suggesting that respiratory phase affected some of the network measurements in only part of the predefined network thresholds (phase × measurement × average density, $F(8,224) = 2.38$, $P = 0.017$,

partial $\eta^2 = 0.078$, 90% CI $= 0.007 \leq \eta \leq 0.108$). Follow-up analyses revealed that the respiratory phase drove changes in network connectivity in the theta (Fig. 2b–d) and beta1 (Fig. 2e,f) ranges. Specifically, in the theta range, we observed that nasal inhalation drove a reduction in the mean local efficiency (average density = 15, inhale = 0.733 ± 0.058, exhale = 0.765 ± 0.050, $P = 0.0021$, Cohen's $d = -0.58$, 95% CI $= -1.10 \leq d \leq -0.07$; average density = 20, inhale = 0.787 ± 0.039, exhale = 0.811 ± 0.028, $P = 0.0055$, Cohen's $d = -0.70$, 95% CI $= -1.22 \leq d \leq -0.18$) and clustering coefficient (average density = 15, inhale = 0.611 ± 0.038, exhale = 0.637 ± 0.036, $P = 0.0039$, Cohen's $d = -0.69$, 95% CI $= -1.21 \leq d \leq -0.17$; average density = 20, inhale = 0.658 ± 0.033, exhale = 0.679 ± 0.03, $P = 0.03$, Cohen's $d = -0.66$, 95% CI $= -1.18 \leq d \leq -0.14$). Yet in the beta1 range, we observed that nasal inhalation drove a reduction in global efficiency (average density = 25, inhale = 0.660 ± 0.02, exhale = 0.672 ± 0.01, $P = 0.024$, Cohen's $d = -0.75$, 95% CI $= -1.27 \leq d \leq -0.23$; average density = 30, inhale = 0.717 ± 0.017, exhale = 0.728 ± 0.012, $P = 0.007$, Cohen's $d = -0.74$, 95% CI $= -1.26 \leq d \leq -0.21$) with an increased mean strength (average density = 25, inhale = 38.82 ± 3.75, exhale = 37.37 ± 3.19, $P = 0.034$, Cohen's $d = 0.41$, 95% CI $= -0.10 \leq d \leq 0.92$; average density = 30, inhale = 44.68 ± 4.92, exhale = 42.66 ± 4.14, $P = 0.027$, Cohen's $d = 0.44$, 95% CI $= -0.07 \leq d \leq -0.95$). The specific effects are detailed in Supplementary Table 1, and the electrodes primarily responsible for these shifts are identified in Supplementary Fig. 2. Had shifts occurred in low respiratory frequencies, one could perhaps dismiss them as respiratory artefacts, yet shifts in the theta (clearly visualized in the comparison of the top and bottom panels of Fig. 2b) and beta1 ranges are consistent with an effect on brain mechanisms related to attention[34]. This is consistent with our notion of inhalation driving a stimulus-processing phase. If the brain indeed enters a generalized stimulus acquisition phase on inhalation, one would expect that the same stimulus would then be processed differently on inhalation versus exhalation, resulting in different behaviour and different brain activity. Thus, we continued with addressing these questions.

Inhalation at task onset is associated with improved visuospatial performance. We first set out to quantify behaviour during the task. To verify that the system automatically triggered trials at the intended respiratory phase, we plotted the respiratory trace aligned with trial onset. We observed a clear separation of inhale and exhale trials (mean visuospatial: phase at onset inhale = −1.43 ± 0.3 rad, exhale = 1.85 ± 0.71 rad; lexical: phase at onset inhale = −1.45 ± 0.27 rad, exhale = 1.87 ± 0.55 rad, Watson–Williams circular one-factor ANOVA (test for the equality of means in circular data), both $P < 0.001$) (Fig. 3a). We then examined performance in the tasks as a function of respiratory phase. A repeated-measures ANOVA on accuracy with conditions of task (visuospatial or lexical) and phase (inhale or exhale) revealed a main effect of task ($F(1,27) = 67.44$, $P < 0.001$, partial $\eta^2 = 0.078$, 90% CI $= 0.007 \leq \eta \leq 0.108$), reflecting that the lexical task was easier than the visuospatial task (mean visuospatial: 71.11 ± 10.69%; mean lexical: 88.61 ± 7.11%, two-tailed paired t-test $t(28) = 8.4$, $P < 0.001$, Cohen's $d = -1.93$, 95% CI $= -2.54 \leq d \leq -1.26$), a main effect of phase ($F(1,27) = 7.35$, $P = 0.012$, partial $\eta^2 = 0.021$, 90% CI $= 0.029 \leq \eta \leq 0.405$), reflecting a better overall performance in inhalation over exhalation (mean inhale: 80.52 ± 6.80%, mean exhale: 78.86 ± 7.42%, two-tailed paired t-test $t(28) = 2.54$, $P = 0.017$), and a significant interaction between task and phase ($F(1,27) = 22.65$, $P < 0.001$, partial $\eta^2 = 0.456$, 90% CI $= 0.208 \leq \eta \leq 0.606$), reflecting a dissociation of a significant advantage in performance during inhale over exhale in the visuospatial task (mean visuospatial: inhale: 73.27 ± 10.91%; exhale: 68.04 ± 11.32%, two-tailed paired t-test $t(28) = 4.49$, $P < 0.001$, Cohen's $d = 0.47$, 95% CI $= -0.08 \leq d \leq 1$) (Fig. 3b,c) (this effect also increased as the task progressed; Supplementary Fig. 3), yet a trend towards advantage in performance during exhale over inhale in the lexical task (lexical: inhale: 87.8 ± 7.6%; exhale: 89.7 ± 7.8%, Wilcoxon signed-rank, $Z = 1.59$, $P = 0.11$, Cohen's $d = 0.23$, 95% CI $= -0.79 \leq d \leq 0.3$, if tested parametrically: two-tailed paired t-test $t(27) = 2.18$, $P = 0.038$) (Fig. 3d).

The effect of nasal inhalation on visuospatial task accuracy was striking (Fig. 3b) to the extent that we sought to replicate it before continuation. In experiment 3, 18 new participants (13 women, age = 24.94 ± 3.7 years) conducted the 160-trial version of the respiratory-triggered visuospatial task. We again observed that trials were correctly triggered in accordance with respiratory phase (Supplementary Fig. 4a). Moreover, consistent with experiment 2, we observed that performance was again significantly better in trials triggered by inhalation than in trials triggered by exhalation (mean % accuracy inhale: 72.04 ± 9.80%; exhale: 69.24 ± 8.57%, Wilcoxon signed-rank, $Z = 2.28$, $P = 0.022$, Cohen's $d = 0.30$, 95% CI $= -0.36 \leq d \leq 0.95$; if tested parametrically: two-tailed paired t-test: $t(17) = 2.37$, $P = 0.03$) (Supplementary Fig. 4b). In other words, experiment 3 replicated the behavioural results of experiment 2.

In experiment 4, we further asked whether this phenomenon was restricted to nasal inhalation alone or whether it also persists in oral inhalation. We repeated the above task again with a new cohort of 18 participants (12 women, age = 25.82 ± 2.61 years), but prevented nasal respiration with a nasal clip. We observed a similar outcome: significantly better performance following oral inhalation versus exhalation (mean % accuracy inhale: 74.00 ± 7.72%; exhale: 69.74 ± 7.51%, Wilcoxon signed-rank, $Z = 1.98$, $P = 0.047$, Cohen's $d = 0.55$, 95% CI $= -0.12 \leq d \leq 1.21$; if tested parametrically: two-tailed paired t-test $t(17) = 2.37$, $P = 0.029$) (Supplementary Fig. 4c,d). Whereas the effect of respiratory phase on visuospatial performance was robust and now replicated, the effects on lexical decision making were not significant, and were in fact trending in the opposite direction. To further verify this result, in experiment 5, we replicated the lexical decision task in 30 additional participants (16 women, age = 25.7 ± 3.3 years) and observed again that respiratory phase had no effect on performance in the lexical decision task (mean % accuracy inhale: 90.18 ± 10.89%; exhale: 89.91 ± 10.22%, Wilcoxon signed-rank, $Z = 1.35$, $P = 0.176$, Cohen's $d = 0.12$, 95% CI $= -0.39 \leq d \leq 0.62$; if tested parametrically: two-tailed paired t-test $t(29) = 1.74$, $P = 0.0918$). In experiment 5, we also added an explicit questionnaire that further verified that participants were unaware of our interest in nasal airflow; see Supplementary Fig. 5. Taken together, we conclude that the spontaneous tendency to inhale at task onset (Fig. 1) probably drove changes in brain network organization (Fig. 2), and this was associated with a pronounced improvement in performance in the visuospatial task (Fig. 3). We next set out to ask where and how this phase-specific performance was reflected in brain activity.

Nasal inhalation drives task-specific increased local brain activity in non-limbic regions. We probed for differences in the brain-evoked response to the same cognitive task, either visuospatial or lexical, as a function of respiratory phase, either inhale or exhale. Consistent with the non-significant behavioural effect in the lexical decision task, we failed to observe significant differences in brain activity between inhale and exhale in this task (Supplementary Figs. 6 and 7). By contrast, in the visuospatial task, we observed a significant main effect of respiratory phase in a time window of 185–270 ms post-stimulus onset (topographical ANOVA (tANOVA) maximum–minimum, $P = 0.0026$, Cohen's d analogue = 3.04) (Fig. 4a). Topographical estimation of scalp current densities revealed that the largest increase in positivity occurred at frontal electrodes (minimum t-value at electrode FC5, t-value = −3.516) (Figs. 4b,c and 5a), and the largest increase in negativity occurred at parieto-occipital electrodes

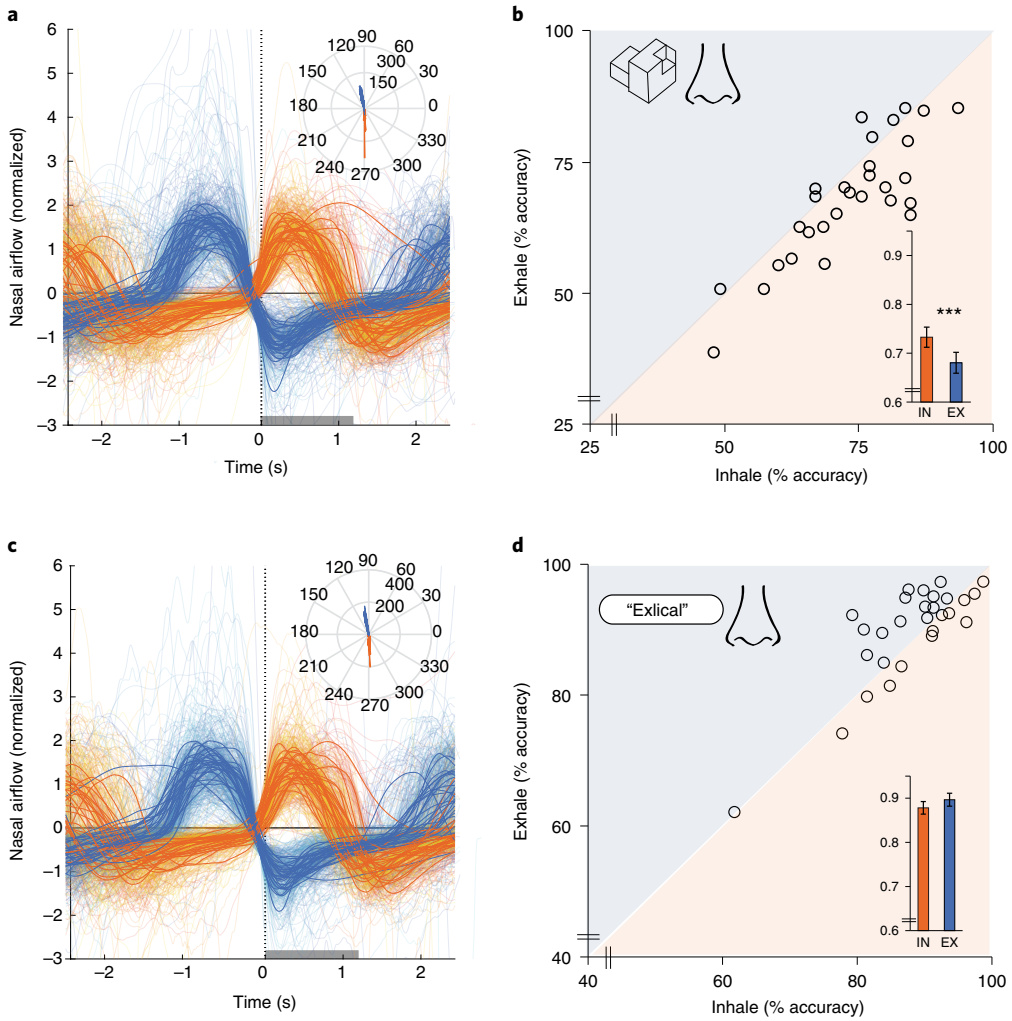

Fig. 3 | Nasal inhalation at visuospatial task onset is associated with improved performance. a, Mean event-related nasal respiratory signal used to trigger trial-onset time-locked to inhalation (orange) or exhalation (blue). Time 0 denotes task initiation. The thick traces are per-subject means and the fine lines are individual trials (to limit clutter, only every fifth trial is plotted per condition). The grey rectangle along the *x* axis represents the stimulus (1,200 ms). Inset: a polar plot of the respiratory phase (in degrees) at trial onset is shown. The orange and blue bins are trials triggered by inhalation and exhalation, respectively ($n=28$). **b**, Scatter plot of performance in the EEG visuospatial task in inhalation and exhalation. Each point is a participant ($n=28$). The diagonal line is the unit slope line ($x=y$). Thus, if points accumulate below the line, performance was better during inhale. In the inlay, the mean group performance is shown. Error bars are s.e. Two-tailed paired *t*-test, ***$P=0.001$. **c**,**d**, Same as **a** and **b**, respectively, but during the EEG lexical decision task ($n=27$).

(maximum *t*-value at electrode P4, *t*-value = 3.058) (Figs. 4b,c and 5b). To address this within a full factorial design, we entered peak event-related potential (ERP) responses within this time window into a repeated-measures ANOVA with conditions of task (visuospatial or lexical), electrode (P4 or FC5) and respiratory phase (inhale or exhale). We observed a main effect of electrode (which is to be expected given the opposite directions of the negative and positive components observed) ($F(1,26)=55.28$, $P<0.001$, partial $\eta^2=0.680$, 90% CI = $0.474\leq\eta\leq0.772$), a marginal interaction of electrode × phase ($F(1,26)=3.89$, $P=0.059$, partial $\eta^2=0.130$, 90% CI = $0\leq\eta\leq0.323$) and, critically, a triple interaction of electrode × task × phase ($F(1,26)=5.80$, $P=0.023$, partial $\eta^2=0.182$, 90% CI = $0.014\leq\eta\leq0.377$), reflecting modulation of both parieto-occipital and frontal ERP amplitudes by respiration in the visuospatial task but not in the lexical task (peak visuospatial: P4 inhale: $-2.42\pm1.66\,\mu V$, P4 exhale: $-1.53\pm1.67\,\mu V$, FC5 inhale: 1.27 ± 1.01; FC5 exhale: $0.89\pm1.43\,\mu V$; lexical: P4 inhale: $-2.02\pm1.49\,\mu V$, P4 exhale: $-2.19\pm1.82\,\mu V$, FC5 inhale: 1.78 ± 1.09; FC5 exhale: $1.90\pm1.21\,\mu V$,). No other main effects of interactions were observed (all $P>0.087$).

In addition, the tANOVA revealed a second significant time window of 915–975 ms post-stimulus onset (tANOVA maximum–minimum, $P=0.003$, Cohen's *d* analogue = 1.41) (Fig. 4a). Topographical estimation revealed that the largest increase in negativity occurred in this later time window at occipital electrodes (maximum *t*-value at electrode O2, *t*-value = 3.614), and the largest increase in positivity occurred at frontal electrodes (minimum *t*-value at electrode F2, *t*-value = −3.872) (Supplementary Fig. 9). To again address this within a full factorial design, we entered peak ERP responses within this time window into an ANOVA with conditions of task (visuospatial or lexical), electrode (O2 or F2) and respiratory phase (inhale or exhale). We observed a main effect of electrode ($F(1,26)=13.17$, $P=0.0012$, partial $\eta^2=0.336$, 90% CI = $0.10\leq\eta\leq0.513$), but no other significant main effects or interactions (all $P>0.076$). Whereas this later, non-task-specific source may be related to various late-phase aspects of the task, such as

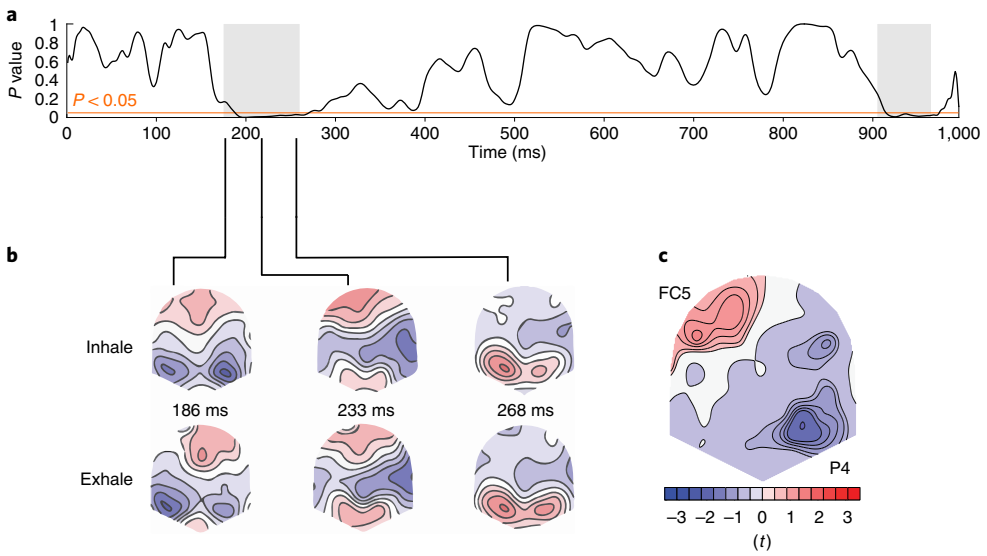

Fig. 4 | Nasal inhalation drives task-specific increased local brain activity in non-limbic regions. a, Point-by-point plot of the tANOVA *P* value comparing inhalation and exhalation task-induced ERP over time ($n=25$). The grey rectangles around 200 and 900 ms post-stimulus onset denote significant consecutive time points. **b**, Excerpts of ERPs mapped onto scalp topography within the window of the main effect (start (186 ms), middle (233 ms) and end (268 ms)) during inhalation and exhalation. The nose is at the top and the apex is the inion (Iz) electrode. **c**, Topographical map of the tANOVA main effect comparing respiratory-phase-coupled ERP activity. Inhalation-coupled increased negativity is shown in blue and inhalation-coupled increased positivity is shown in red. Frontal and parietal foci originate from the location of electrodes FC5 and P4, respectively.

the motor response or ensuing self-appraisal, the early sources fall squarely within stimulus-processing time frames, with the negative and positive deflections corresponding to the well-characterized N200 (ref. [35]) and P200 (ref. [36]) ERP components, respectively. Importantly, a contrast of inhalation versus exhalation without concurrent task trials showed no difference in these electrodes or ERP components (the critical time-window duration was 42.9 ms, and the maximal observed time window was 279–283 ms post-phase onset; Supplementary Fig. 10). Moreover, a separate analysis implied that the N200 and P200 results were not merely reflections of performance accuracy (Supplementary Fig. 11). Thus, we conclude that the exact same cognitive task and stimuli are associated with increased brain response within localized regions (in non-olfactory cortical substrates) if they are encountered in inhalation versus exhalation.

To further probe the link between the behavioural pattern and the brain activity pattern that we observed, we asked whether greater differences in performance between inhale and exhale were associated with greater differences in activity across conditions within the time window uncovered by the tANOVA (185–270 ms). We hypothesized that such a relation, if evident, should be in the vicinity of P4 and/or FC5. To reduce the possibility of reporting spurious correlations, we probed for locations with two or more contiguous electrodes significantly correlated with behaviour. We observed only one such location where two contiguous electrodes were significantly negatively correlated with behaviour, and these two electrodes were indeed immediate neighbours of FC5 (FT7: $r=-0.468$ $P=0.018$, 95% CI $=-0.728\leq r\leq-0.09$; T7: $r=-0.477$, $P=0.016$, 95% CI $=-0.733\leq r\leq-0.101$) (Fig. 5c,d and Supplementary Fig. 12). To further verify that this was indeed not a spurious result, we first pooled the signal from these two electrodes and observed that the negative correlation was preserved (FT7 + T7: $r=-0.524$, $P=0.007$, 95% CI $=-0.761\leq r\leq-0.163$). Next, using the spatial location of the electrodes in the head cap, we estimated the distance between the adjacent FT7 and T7 at 27.29 mm. We then reiterated the correlation analysis for every possible pair of adjacent electrodes located 25–30 mm apart, totalling at 48 pairs (Fig. 5e). The absolute correlation between the joint signal recorded over FT7 and T7 ranked highest among the 48 comparisons (Fig. 5f). We also calculated the correlation between behavioural results and every possible pair of electrodes on the head cap (Fig. 5g). Out of 2,016 such pairs, FT7 and T7 ranked second (Fig. 5h). The electrode pair that ranked first ($r=-0.598$, $P=0.002$, 95% CI $=0.105\leq r\leq0.735$) was non-adjacent FCz and C5—an electrode juxtaposed with T7. In other words, these analyses imply that the correlation between the respiratory-coupled ERP signal and task performance is genuine. Finally, we also observed a single electrode at a different location with a significant positive correlation (C1: $r=0.48$, $P=0.015$, 95% CI $=-0.803\leq r\leq-0.266$), but we cannot determine with confidence that this lone electrode was not spurious.

To further probe for respiratory-phase-dependent alterations in brain response during task performance, we used standardized low-resolution brain electromagnetic tomography (sLORETA), which provides three-dimensional tomography maps[37]. We observed that trials presented during nasal inhalation versus exhalation were associated with significant localized decreases in EEG alpha and beta1 power. More specifically, during trials in inhalation, EEG alpha power was significantly reduced in the right postcentral gyrus (peak value $t=-4.90$, $P=0.017$, MNI (Montreal Neurological Institute) coordinates $x=60$, $y=-30$, $z=45$, Brodmann area 2 (BA2)) and the right parahippocampal gyrus (peak value $t=-4.76$, $P=0.017$, MNI coordinates $x=20$, $y=-25$, $z=-20$, BA35) (Fig. 6a). In addition, during trials in inhalation, EEG beta1 power was significantly reduced in the left precuneus (peak value $t=-5.46$, $P=0.0025$, MNI coordinates $x=-10$, $y=-60$, $z=20$, BA31) (Fig. 6b). In turn, we saw no evidence for respiratory-phase differences in these regions and frequencies in equivalent time epochs without concurrent task trials (t-value at the postcentral gyrus peak coordinate: $t=0.26$, t-value at the parahippocampal gyrus peak coordinate: $t=0.21$, t-value at the left precuneus peak coordinate: $t=1.58$, all $P>0.38$; Supplementary Fig. 13). As to the source localization of these effects, one must always keep in mind the limitations of EEG in this respect[38,39]. That said, these results in the parahippocampal

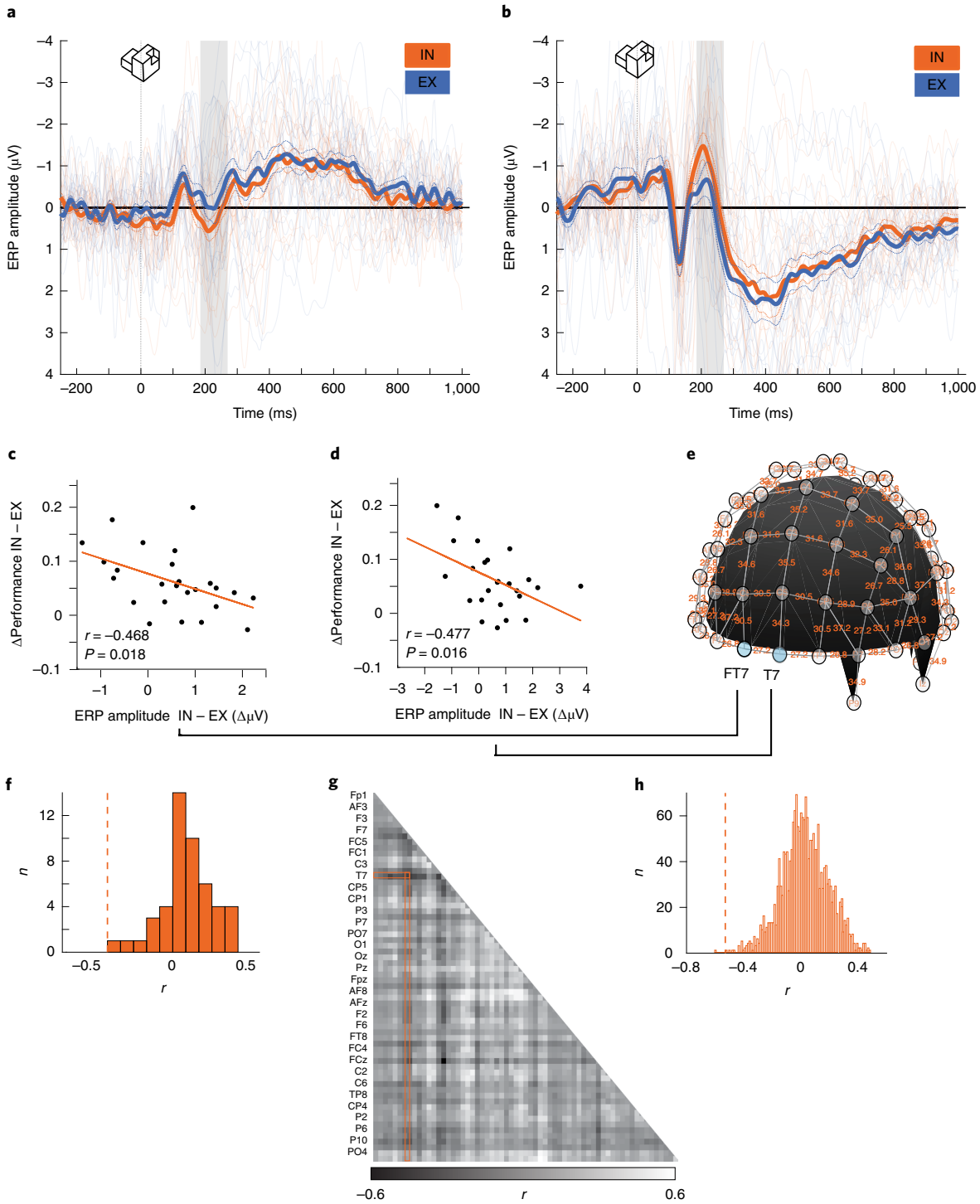

Fig. 5 | Respiratory-phase-locked shifts in neural activity are correlated with phase-locked shifts in behavioural performance. a,**b**, Grand mean ± s.e. of respiratory-phase-coupled ERP traces evoked by visuospatial trials presented during inhalation and exhalation recorded from FC5 (**a**) and P4 (**b**) ($n = 25$). The dashed black line at time zero denotes task onset. Negative values are plotted upwards. The grey rectangle is the tANOVA main effect. **c**–**e**, Scatter plots of correlation between phase dependence in ERPs and phase dependence in behavioural performance in electrodes FT7 (**c**) and T7 (**d**). Each point is a participant ($n = 25$). The orange line is the linear fit. Pairwise distances of all electrode pairs sharing similar distance with that of FT7 and T7 (highlighted in light blue) are also shown (**e**). **f**, Histogram of r values of all two-electrode pairs sharing similar distance with FT7 and T7. The dashed orange line represents the value of the actual data. **g**, Correlation (r values) of the differential ERP signals pooled from every electrode pair combination and the delta of behavioural performance. The white and black hues represent the magnitude of positive and negative correlations, respectively. Note the dark shades joining FT7 and T7 (orange boxes). **h**, Histogram of r values of all possible two-electrode pairs. The dashed orange line represents the value of the actual data.

gyrus and precuneus are precisely overlapping with the PET imaging results obtained using the same paradigm[32], lending credibility to the patterns that we observed. Thus, using an additional measure, we again observe that the exact same cognitive task and stimuli are associated with altered brain response within localized regions if they are encountered in inhalation versus exhalation.

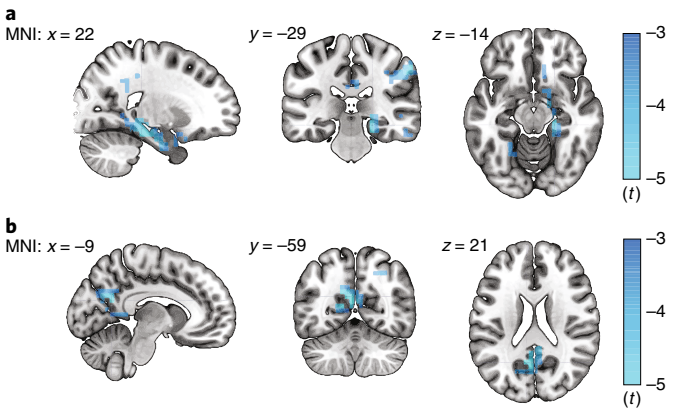

Fig. 6 | Nasal inhalation drives localized task-specific reductions in EEG power. a, sLORETA source localization *t*-maps of ERPs in the visuospatial task phase-locked to inhalation and exhalation onset within the alpha frequency band (8–12 Hz) ($n = 27$). Volumetric data are centred around coordinates of the highest *t*-value in the MNI space. The colour map depicts lower alpha and beta1 power in inhalation versus exhalation (hence the negative values). The brighter shades of blue represent greater reductions. There were no significant increases. **b**, Same as **a**, but for the beta1 frequency band (12–16.5 Hz) ($n = 27$).

Inhale–exhale differences in resting brain connectivity reflected later inhale–exhale differences in performance accuracy. Nasal respiration at rest drove changes in the functional connectivity-derived network architecture, with different patterns associated with inhalation and exhalation. This change in network architecture may underlie respiratory-phase-specific differences in behaviour and neural activity that we observed during the task. To probe the link between these observations, we asked whether the baseline network shifts were related to later shifts in performance at the individual participant level. We generated a simple linear model (see the 'Classifier modelling' section in Methods) that related the difference in network connectivity between inhalation and exhalation at rest to the later performance differences in inhalation versus exhalation. We built the model on 18 participants and tested it on the remaining 10 participants, and repeated this process 10,000 times. We observed that the average correlation between predicted and actual performance differences was $r = 0.32 \pm 0.3$. To estimate the significance of this outcome, we repeated the analysis 5,000 times, each time randomly reassigning performance scores, and observed an average $r = -0.01$ and, moreover, that the real data fell within the top 3% of random permutations (Fig. 7a–c). As a further test of this result, we applied the same modelling scheme in an effort to predict performance in the lexical decision task, and failed ($r = -0.12$, ranked 76th out of 100 random permutations). In other words, the predictive power for the visuospatial task seems modest but genuine. We note that the model relied primarily on features extracted in the theta frequency domain (Fig. 7d). Finally, to verify that our model did not merely capture inter-subject variability in baseline cognitive abilities, we re-ran an identical predictive pipeline, but now tried to predict absolute performance rather than performance differences between inhale and exhale. We observed an average correlation of $r = -0.03$, suggesting no link between baseline respiratory-phase-dependent network properties in EEG and absolute performance level. Thus, we conclude a genuine link between inhale–exhale differences in neural activity at rest and later inhale–exhale differences in behavioural performance at a visuospatial task.

Discussion

The Oxford Dictionary tells us that inspiration is both 'the drawing in of breath' and 'the process of being mentally stimulated' or 'a sudden brilliant, creative, or timely idea'. Our data indicate that this implied link between respiratory phase and mentation is no coincidence. A substantial body of evidence implied that respiration affects rodent[15–18,21–23,26] and human[6,14,19,27,28] brain activity patterns. However, the reported effect of this on human behaviour consisted of mostly static effects following continuous alterations in the dynamic respiratory cycle. For example, people can adapt more regular and deliberate breathing patterns to modify cognitive state and reduce stress[40]. In turn, more transient respiratory-phase-dependent effects were restricted to behaviours that depend on ventral temporal rhinencephalic substrates[27–30]. Here, rather than an overall change in breathing pattern that leads to an overall change in cognition, we identified a respiratory-phase-specific effect on non-limbic cognition that changes breath-by-breath. Performance at a visuospatial task was enhanced during inhale, reduced during ensuing exhale and enhanced again during ensuing inhale. Moreover, although participants were unaware of this link, it nevertheless subliminally affected their behaviour, as evidenced by their implicit tendency to opt for trial onset upon inhale. Finally, the EEG data implied that the brain indeed processes the same stimulus differently when encountered during inhale or exhale, and that this difference was evident in non-limbic task-specific areas of processing.

Can the EEG data provide for a more mechanistic interpretation? We observe that the resting-state analysis implied shifts in connectivity between inhale and exhale. Given the role attributed to shifts in connectivity in the repertoire of functional brain response patterns[41], this respiratory-phase-dependent shift in topology is meaningful by itself. But what are the specific implications of these specific shifts in topology? In beta1, we observed increased mean strength, an effect stemming primarily from electrode CP4 (Supplementary Fig. 2). Increased mean strength in beta1 in parietal regions is consistent with increased attention[42], hence this result is consistent with our overall view of an information-gathering state at inhale. In turn, the combination of reduced global efficiency in beta1 and reduced mean local efficiency and clustering coefficient in theta together point to a state of brain connectivity with reduced small-worldness[43]. In the EEG of cognition, the extent of small-worldness is typically compared between populations (for example, impaired versus unimpaired) or between semi-static states (on versus off a drug), and in such instances, reductions in small-worldness are typically associated with negative outcome[44,45]. Here, however, we estimate small-worldness not across individuals in static states, but rather within individuals in a dynamic process (respiration), and observe reductions in small-worldness associated with what we consider the higher attentive state. In this respect, we note that, in the context of a dynamic task, small-worldness is indeed reduced with attentional task (go–no go) onset[46].

Next, when we then look at the EEG evoked response during the task (rather than connectivity at rest), we observed that trial-related parieto-occipital N200 and frontal P200 were significantly larger during inhale versus exhale. A parieto-occipital N200 is consistent with processing visuospatial information[35], and a frontal P200 is consistent with hierarchical selection of task-relevant features inherent to this particular task[36]. Moreover, when using a global frequency-dependent approach rather than a local amplitude-related measure, we observed task-specific reductions in alpha and beta1 power, the former in the right postcentral and parahippocampal gyri, and the latter in the left precuneus. Reductions in alpha power are associated with desynchronization and high excitability during task performance[47]. In this sense, the task-related reductions that we observed are consistent with the literature and probably reflect aspects related to the button pressing associated with the task (postcentral gyrus)[48] and the need to distinguish between relevant and irrelevant landmarks within a visuospatial effort[49].

Thus, taken together, the EEG data imply a model in which inhalation prepares the brain for incoming sensory information

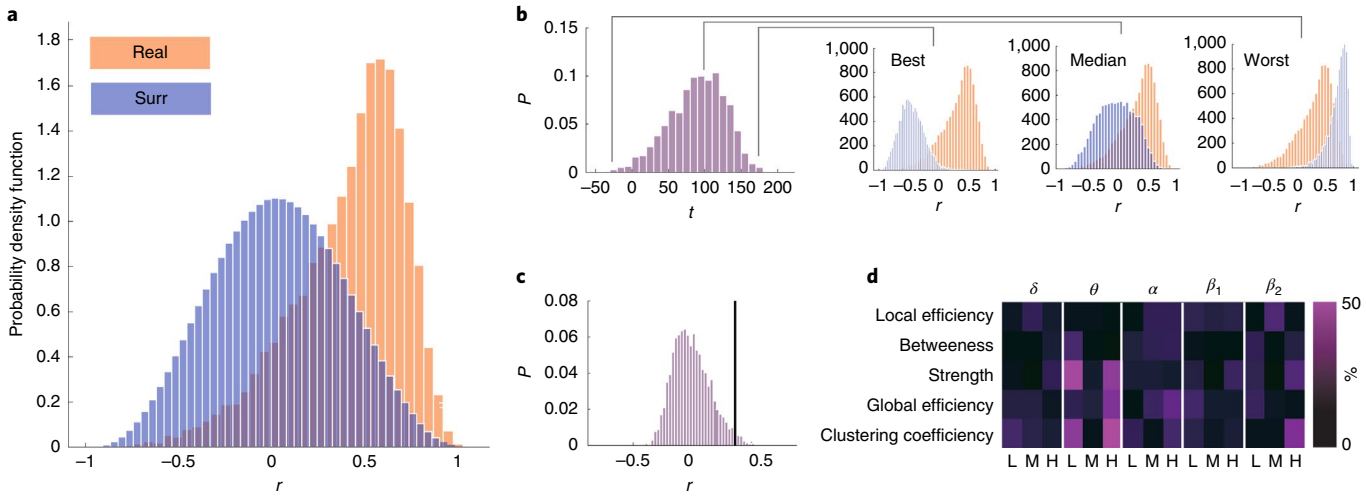

Fig. 7 | Inhale–exhale differences in resting brain connectivity reflected later inhale–exhale differences in performance accuracy. a, Correlations between neural activity and behavioural performance in the model (orange) and 5,000 control shuffles (blue) (see Methods). **b**, Statistical comparison (*t*-test) between the real data (orange in **a**) and all of the possible shuffles (blue in **a**). Inlays are the best, intermediate and worst cases of difference between real and shuffled data. **c**, Histogram of the average *r* in shuffled data (blue in **a**), with the real *r* (orange in **a**) denoted by the black line. **d**, Network feature importance derived from lasso feature selection (see Methods). Features are sorted in a matrix according to measurement type (rows) and frequency band (columns), each further divided into three bins of low (L), medium (M) and high (H) predefined average density. The colour codes the number of times each feature was selected for the 10,000 partitions of the real data; brighter colours denote higher values of selection.

(as implied in the beta1 mean strength), and once this is acquired, inhalation further optimizes neural processing in task-specific neural substrates (as evidenced in the ERP). A remaining critical question is of course what is driving all of this? The most likely answer is a common internal driver for inhalation and orchestrated patterns of brain activity. We can speculate that such a driver may be located in the pre-Bötzinger complex[22,50] and may involve amygdaloidal connectivity[51,52]. In turn, and despite the results of our oral control (Supplementary Fig. 4d), the possibility of external modulation from sensation of actual respiratory airflow should not yet be abandoned[20].

This study was inspired by an evolutionary hypothesis. Evolutionary hypotheses cannot be directly tested and data can only be consistent or inconsistent with their gist. Beyond data consistent with an evolutionary hypothesis, we uncovered a mechanism reflecting a potentially primary feature of interplay between bodily physiology, the brain and cognition: inhalation-phase mentation. We propose that inhalation drives patterns of neural activity consistent with heightened attention, thus optimizing processing of incoming information of all kinds. Beyond theoretical impact alone, our results may provide implications on several fronts. One such front is learning. Our results suggest a respiratory phase that is optimal for stimulus acquisition. This may imply novel learning strategies in which acquisition is phase-locked with respiration. A second area of immediate implication is in the design and analysis of human brain imaging studies, particularly using fMRI. Because the fMRI signal is dependent on oxygenation and levels of CO_2, respiration is treated in fMRI primarily as a source of physiological noise, and there are extensive measures applied to removing this noise from the signal[53]. Our results imply that participants may modulate their respiration to match the task and that respiration then optimizes task-specific neural activity. Thus, by 'cleaning out' respiration, fMRI studies may be cleaning out a very important source of genuine variance in brain function. This may have had a significant effect on the interpretation of cognitive function using fMRI. Alas, we see no easy way around this. Respiration is undeniably a potential source of physiological noise in fMRI, yet it is also likely a genuine orchestrator and driver of neural activity in cognitive tasks.

Finally, we would like to acknowledge several limitations of this study. First, owing to technical limitations, our EEG did not include the gamma or high gamma frequency domains. Given that these frequencies have been associated with attentional mechanisms and their possible relation to respiration[27], this implies that there may be effects that we are missing in our analyses. Second, the effect that we predicted did not materialize in the behaviour or ERP of the lexical task. We can see two alternative methodological explanations for this lack: first, there may be interference between respiration and silent mouthing or subvocalization in the lexical decision task, and second, the lexical task was significantly easier than the visuospatial task, introducing a possible ceiling effect, potentially obscuring the impact of inhalation. In turn, the difference between the lexical and visuospatial tasks may be genuine. Indeed, modality specificity was previously observed in the effect of nasal inhalation on mental imagery[28]. All of this suggests that we cannot conclude that our hypothesis of an overall stimulus acquisition phase of brain processing equally applies to all modalities and tasks. Indeed, if one considers the variance in the data, it may also not equally apply to all individuals. In other words, we can foresee an ultimately more complex picture emerging in which some tasks are 'inhale tasks' and others are 'exhale tasks', and, moreover, that some individuals are 'inhalers' and others 'exhalers'. Although these possible sources of variance implicate various directions for future research, the flip side of this is that the lexical task provided an extensive EEG control condition in this study. Most EEG concerns that we could think of were mitigated by the fact that a different task with the same number of trials, the same temporal design and in the same participants did not yield effects. In this respect, the lack of effects in the lexical task was a bug-turned-feature in this effort. A third limitation of our results was that, in contrast to our prediction, the effect of respiratory phase on performance was similar for oral and nasal inhalation. A 'picture perfect' result consistent with our overarching hypothesis would have been an effect in nasal but not oral inhalation. Although we did not observe such a 'picture perfect' pattern, the pattern that we did observe does not negate our hypothesis. Under natural circumstances, oral and nasal inhalations occur either in concert, or nasal inhalation alone (inhaling with a closed mouth). The condition

of oral inhalation alone is unnatural and is largely restricted to the disease state of a completely stuffed or blocked nose, or the artificial experimental state of a clipped nose, as was the case here. It is unsurprising that the brain did not evolve to account for these two conditions. Thus, given that inhalation, whether nasal or oral, is driven by common brain substrates[22,50–52], it is not unreasonable that a stimulus-processing mode triggered by inhalation would remain triggered by oral inhalation alone. Finally, this paper contains many experiments and analyses. The advantage of this is that we tested our hypothesis from many angles, and this converged towards a common answer. The flip side of this is that the large number of tests increases the chances of noise from random sampling. To address this, we took a meta-analysis approach using *P*-curve analysis[54], and this indicated an overall evidential value of our results (Supplementary Fig. 15). Nevertheless, this issue should remain in mind.

Although the above limitations deserve attention, we think that they do not take away from our main conclusions. The combination of the spontaneous tendency to nasally inhale at task onset, the better performance at inhale and the altered brain response during inhale that is correlated with performance, all point to a respiratory-phase-dependent mode of processing, or in other words, a sniffing brain[55]. This finding of mental processes with no link to olfaction that are nevertheless phase-locked with nasal inhalation is consistent with our hypothesis of a functional olfaction-based template in human brain evolution.

Methods

Participants. Written informed consent to procedures approved by the Weizmann Institute International Review Board Committee was obtained from all participants. Participants were all native Hebrew speakers, in general good health, with normal or corrected-to-normal vision, and reported no history of neurological or mental illness, attention deficit disorders or dyslexia. Participants were instructed not to ingest caffeinated beverages up to 2 h before experimentation. Additional exclusion criteria were any chronic or acute conditions that involved the respiratory tracts. All participants were paid for their participation. Participants were blind to the experimental goals and interests, experimenters were not. As to the number of participants, we could not start with a formal power analysis, as previous similar studies did not include the raw data necessary for estimating correlation across conditions. Thus, we recruited 30 participants per condition, that is, a cohort similar in size to previous studies of this type[27]. For the internal replication experiment, we conducted power analysis using G*Power software[56], which indicated that for power = 0.8, we need to recruit $n = 18$.

Experiment 1: measuring nasal airflow concurrent with cognitive tasks. Thirty-one individuals participated in this experiment (15 women, mean age = 25.67 ± 2.27 years) in which we measured nasal airflow during performance of cognitive tasks. In this and all ensuing experiments, we relied on methods that we have used extensively in the measurement and characterization of nasal airflow[57]. Nasal respiration was sampled at 100 Hz using a nasal cannula linked to a spirometer (ML141, ADInstruments) and Power-Lab 16SP Monitoring System (ADInstruments). To draw attention away from respiratory monitoring, we used the same recording setup to also acquire heart rate via a finger pulse sensor, which was fitted to the first phalanx of the index finger of the left hand. Technical faults corrupted some data, retaining 24, 29 and 26 participants for analysis in the mathematical, visuospatial and lexical decision tasks, respectively. For analysis, the normalized respiratory signal was collapsed across trials, resulting in a mean respiratory trace per participant, time-locked to the time of trial onset. To assess the salience of the respiratory response to task onset, as well as its deviation from baseline signal fluctuations, we applied the following statistical pipeline: sign proportion per trial, defined as the sum of the positive sign values (regardless of magnitude) of the respiratory signal within a time window was calculated and averaged across trials per participant. We then applied circular permutation to the entire respiratory trace to extract the same parameter of sign proportion from random points during the session (trial onsets were fixed). As with the task data, values were averaged across trials per participant. Finally, the mean respiratory sign proportion at task onset was compared with the mean surrogate data per participant in a paired *t*-test. In other words, surrogate time points were randomly selected and their duration was set to match the actual task data. We reiterated this process for time windows of incremental duration from the time of task onset onwards. The MATLAB code for this analysis can be found in the Code availability.

Experiment 2: EEG. Thirty individuals participated in this experiment (8 women, mean age = 25.8 ± 2.8 years) in which trials were triggered by nasal respiration, here concurrent with EEG recordings. We used standard methods typically applied in EEG: continuous EEG was recorded from 64 electrodes embedded in an elastic head cap (BioSemi) arranged according to the extended 10–20 system[58]. Skin was abraded at each electrode site and conductive gel (Signa Gel, Parker) was applied. Vertical eye movement and blinks were monitored with two electrodes placed above and below the right eye, and horizontal eye movements were monitored by an electrode placed at the outer canthi or the left eye (eye data were unavailable for one participant). EEG was also recorded from bilateral mastoid locations, which later served as a linked reference. Impedances were maintained below 25 kOhm. The EEG signal was amplified and digitized at 2,048 Hz by ActiveTwo AD-box (BioSemi), controlled by ActiView 7.02 (BioSemi) data acquisition software.

Following application of the recording electrodes, participants were left alone in the dimly lit room to be monitored from an adjacent control room. Lexical decision and visuospatial tasks were counterbalanced for order across participants, and triggering from inhale or exhale was randomly ordered within participants. The total duration of the experimental session was approximately 80 min (~20 min per movie clip and ~15 min per cognitive task, including breaks).

ERPs. EEG data were analysed using Brain Vision Analyzer 2.0 (Brain Products) with standard methods for EEG ERP derivation: following recording, data were referenced to a mean bilateral mastoid signal post-hoc. Next, data were filtered with a bandpass of 0.5–30 Hz, bandwidth of 0.3 s, 8th order. This low cut-off of 0.5 Hz was selected to remove ongoing respiratory-related artefacts (the respiratory frequency of this data was 0.31 ± 0.08 Hz). In 4 cases, 1 out of 64 electrodes detached mid-experiment. In these cases, it was topographically interpolated from its neighbours using spherical spline interpolation, 4th order. Next, an ocular correction regression algorithm was applied to remove blinks and eye movement-induced artefacts[59]. Following filtration and artefact correction, data were downsampled to 256 Hz. To generate event-related epochs, data underwent segmentation around task-onset markers (time window: −500 to 1,000 ms post-stimulus) according to condition (inhale or exhale). Epochs that contained artefacts were rejected according to the following standard automatic exclusion criteria: maximal voltage step exceeded 50 μV ms^{-1}, maximal absolute difference exceeded 200 μV within 200 ms, activity lower than maximum – minimum of 0.5 μV within 100 ms. This amounted to excluding 9 ± 6.6 or 3% of trials in the visuospatial task and 4.5 ± 5.9 or 5% of trials in the lexical decision task. Next, epoch data were linearly detrended and a mean signal of −500 to 0 ms served as baseline. Finally, epochs were collapsed over trials to generate the mean ERP over each electrode site per participant. In all cases, the first trial was discarded to account for an element of surprise that may accompany session onset.

Statistical analysis. In all experiments, we first tested the normality of data distribution. In cases in which the data were abnormally distributed, we applied non-parametric statistical tests. However, we also reported the results of a parametric test in parenthesis to retain reporting consistency across the paper.

For tANOVA and post-hoc ERP statistical analyses, we used RAGU software[60]. RAGU is a MATLAB-based assumption-free bootstrap randomization statistics suite. Its strength is chiefly in the maximization of statistical power while minimizing the need for a priori choices of model (for example, areas of interest, time window or frequency band). As a preliminary step, we validated the consistency of ERP topographies across the participant cohort. To test this, we subjected the data to a topographical consistency test of 5,000 permutations provided within RAGU. The topographical consistency test confirmed that under both conditions, common activations were found across participants throughout the entire epoch following trial onset (−200 to 1,000 ms, $P < 0.001$). Prior to permutations, data were re-referenced to average and underwent multidimensional scaling to remove outliers within the RAGU package, with the exclusion threshold set at $P < 0.05$. Randomization parameters were set to 5,000 permutations on the L2 norm (scale to unity variance) of the raw data. In the within-subjects statistical design, 'inhalation' and 'exhalation' were reflected in positive and negative *t*-values, respectively, regardless of subsequent EEG current distributions observed on the scalp. The critical *P* value was set at $P < 0.05$. tANOVA was conducted in a within-participant design with a single condition of respiratory phase (inhale or exhale). tANOVA compares differences between groups versus random permutations, precluding traditional effect-size calculations (in which per-participant measurements are used). Thus, effect sizes were calculated using an analogue of Cohen's *d* from *Z*-scores of scalp topography differences between conditions[61].

sLORETA and EEG source localization. We used the distributed source localization algorithm in sLORETA to generate three-dimensional tomography maps in which the localization of brain signals is preserved with low levels of dispersion[37]. We used the ERP data obtained during the visuospatial task (within a time of 0–1,000 ms post-stimulus onset) as input. We then used the 'EEG to cross-spectrum' function in sLORETA to translate these time series into the frequency domain by means of cross-spectral analysis. We investigated network properties within five discrete frequency bins: delta: 0.5–4 Hz, theta: 4–8 Hz, alpha: 8–12 Hz, beta1: 12–16.5 Hz and beta2: 16.5–24 Hz. The current density within each frequency band was calculated separately using the 'cross-spectrum to sLORETA' function. Following participant-wise normalization, we used a paired-group design to compare epochs that took place during inhalation or exhalation.

Statistical testing was conducted on the log-transformed *t*-statistic values of the data within the sLORETA environment. Statistical non-parametric mapping was used to estimate current density distributions of EEG activity generators. Statistical significance was assessed by defining a critical threshold of $P < 0.05$ (two-tailed, whole-brain corrected), corrected for multiple comparisons by a randomization test with 5,000 permutations. For visualization purposes, *t*-values were projected into MNI space coordinates with a colour palette corresponding to *t*-values. Figures are focused around the coordinates of local maxima.

Network connectivity analysis. We used a graph theory approach[33] to investigate the influence of the respiratory cycle on cortical network connectivity. Briefly, signals acquired from the brain can be represented as a graph—nodes denoting different brain areas (in this case, electrode recording sites) and edges representing functional connectivity. To ask how functional connectivity is modulated by the respiratory cycle, inhalation and exhalation markers were used to segment the continuous 64-electrode EEG obtained during the 20-min baseline movie clip into 1-s epochs that occurred exclusively either during inhalation or exhalation. Given that all inhalations versus all exhalations in this study would amount to an extraordinary amount of data, we initially restricted the data to the best-manageable subset as follows: we rank-ordered individual respiratory cycle durations and removed events under the 25th or above the 75th percentile within each participant. Following these exclusions, we still had in hand about 600 epochs per participant. We then further limited the number of epochs per condition per participant, randomly selecting 200 epochs per condition from across the session (except one very slow breather who ended with 156 epochs). We should stress that this connectivity analysis of the resting-state EEG data is the only place where we applied such data reduction, which was not applied in any of the task-related analyses. EEG time series were sampled at 256 Hz. Network measurements of one subject were extremely skewed, suggesting possible corruption of the data during acquisition and were therefore discarded. We investigated network properties within five discrete frequency bins: delta: 0.5–4 Hz, theta: 4–8 Hz, alpha: 8–12 Hz, beta1: 12–16.5 Hz and beta2: 16.5–24 Hz. On the basis of these data sets, we next constructed graphs as follows: edges were defined using the absolute values of pairwise Pearson correlations applied to all electrode data with no time delay. Next, the correlation matrix was thresholded and all of the edges that did not survive were removed, leaving an undirected binary graph (with the exception of the strength measurement, which relied on the weighted version of the graphs). We used six incremental threshold values of average degree (see below), ranging between 5 and 30 as cut-offs (the distribution of *r* values associated with each cut-off is in Supplementary Fig. 16). The following network matrices were calculated on graphs reiteratively per average density and frequency band:

(1) Strength: nodal strength is defined per node as the sum of all its edges, derived from each node's connectivity matrix. This is the only measurement for which the edges' weights were taken into account. Mean strength is defined as the average over all nodal strengths.

(2) Betweenness centrality: path length is defined as the minimum number of edges that are needed to cross on the way from one node to another. Betweenness centrality is therefore defined per node as the number of shortest paths that pass through it. This represents the degree of which nodes stand between each other and, as a result, its importance as a hub in the network.

(3) Global efficiency: defined as the average inverse path length.

(4) Local efficiency: defined per node as the global efficiency in the subgraph that includes only this node's neighbours. Mean local efficiency is the average over all of the nodes' local efficiencies.

(5) Clustering coefficient: quantifies per node how likely it is for two of its neighbours to be connected to one another. Mean clustering coefficient is defined as the average over all the nodes' clustering coefficients.

This set of network measurements was selected because it was used before[33], as a set that provides concise information regarding the topology and structure of graph theory-derived networks[33]. The MATLAB code for this analysis can be found in the Code availability.

The effect of respiratory phase on network connectivity measurements was assessed using a nested repeated-measures ANOVA with conditions of frequency band (delta, theta, alpha, beta1 or beta2), respiratory phase (inhale or exhale), network measurement (strength, betweenness, local efficiency, global efficiency or clustering coefficient) and average density bin (5, 10, 15, 20, 25 or 30). Planned post-hoc comparisons were carried out using targeted two-tailed paired *t*-tests. Finally, to visualize connectivity, we used the BrainNet Viewer suite[62].

Relating phase-specific resting EEG to later phase-specific behavioural performance. To test whether the connectivity measurements are predictive of ensuing task performance, we trained linear classifiers. The classifiers' input was the differences in functional connectivity networks derived during inhale and exhale epochs. The predicted output was the difference in task performance (accuracy) between the inhale and exhale conditions. Both measurements were taken in *Z*-score, and we predicted the *Z*-score of the differences. To estimate our predictions, we performed 10,000 splits of the data into sets of 18 training examples and 10 test examples. Our model was trained on the training set using the lasso method[63]. This resulted in a linear classifier and a list of features selected out of the network measurements pool. Each model was then tested to obtain an *r* value on the 10-participant testing sample. We next performed Fisher *Z*-transformation and averaged the transformed *r* values and inverse-transformed this average, so that we have an estimation on the expected *r* value.

Random permutation test (cross-validation of the linear classifier). To determine whether the correlation values obtained by the linear classifier were statistically significant, we used a randomization approach[64]: we shuffled the performance in the task between subjects randomly, and for each such randomization, we trained a linear classifier and obtained the *r* value of its prediction. Specifically, we took a random permutation of the performance vector and attributed it to the 29 participants. For each randomization, we recomputed the correlation between predicted and actual performance as reported above. The process was reiterated 5,000 times.

Experiments 3–5: triggering tasks from nasal and oral airflow. Sixty-six individuals participated in this series of experiments (41 women, mean age = 25.52 ± 3.2 years) in which trials were triggered by respiration, either inhalation or exhalation. Participants were unaware of this triggering mechanism. In experiments 3 and 4, 18 participants were tested with nasal respiratory triggering, and 18 participants with oral respiratory triggering, respectively. Nasal airflow recording was as in experiment 1, and oral recording used the same devices but linked to a custom silicone mouthpiece. During oral sessions, nasal respiration was prevented using a soft nose-clip. Here, the respiratory recordings were used to trigger trial onset at inhalation or exhalation onset. Trials that were 'misfired', that is, triggered not at inhalation or exhalation onset, were discarded from further analysis. This amounted to an average of 16.7 ± 7.9 trials or approximately 10% of trials. The effect of respiratory phase on performance accuracy and reaction time was analysed using repeated-measures ANOVA followed by two-tailed paired Student's *t*-tests. The MATLAB code for this analysis can be found in the Code availability.

Reporting Summary. Further information on research design is available in the Nature Research Reporting Summary linked to this article.

Code availability

The custom MATLAB scripts used to process and visualize the data collected in this study are available at: https://github.com/WORGOlfaction/perl-2019.

Data availability

The data that support the findings in this study are available from the corresponding authors on request and are also posted at https://www.weizmann.ac.il/neurobiology/worg/materials.html.

Received: 17 August 2018; Accepted: 7 February 2019;
Published online: 11 March 2019

References

1. Craven, B. A., Paterson, E. G. & Settles, G. S. The fluid dynamics of canine olfaction: unique nasal airflow patterns as an explanation of macrosmia. *J. R. Soc. Interface* **7**, 933–943 (2009).
2. Grosmaitre, X., Santarelli, L. C., Tan, J., Luo, M. & Ma, M. Dual functions of mammalian olfactory sensory neurons as odor detectors and mechanical sensors. *Nat. Neurosci.* **10**, 348–354 (2007).
3. Verhagen, J. V., Wesson, D. W., Netoff, T. I., White, J. A. & Wachowiak, M. Sniffing controls an adaptive filter of sensory input to the olfactory bulb. *Nat. Neurosci.* **10**, 631–639 (2007).
4. Shusterman, R., Smear, M. C., Koulakov, A. A. & Rinberg, D. Precise olfactory responses tile the sniff cycle. *Nat. Neurosci.* **14**, 1039–1044 (2011).
5. Smear, M., Shusterman, R., O'Connor, R., Bozza, T. & Rinberg, D. Perception of sniff phase in mouse olfaction. *Nature* **479**, 397–400 (2011).
6. Sobel, N. et al. Sniffing and smelling: separate subsystems in the human olfactory cortex. *Nature* **392**, 282–286 (1998).
7. Fontanini, A., Spano, P. & Bower, J. M. Ketamine-xylazine-induced slow (<1.5 Hz) oscillations in the rat piriform (olfactory) cortex are functionally correlated with respiration. *J. Neurosci.* **23**, 7993–8001 (2003).
8. Kepecs, A., Uchida, N. & Mainen, Z. F. The sniff as a unit of olfactory processing. *Chem. Senses* **31**, 167–179 (2005).
9. Mainland, J. & Sobel, N. The sniff is part of the olfactory percept. *Chem. Senses* **31**, 181–196 (2005).
10. Strausfeld, N. J. & Hildebrand, J. G. Olfactory systems: common design, uncommon origins? *Curr. Opin. Neurobiol.* **9**, 634–639 (1999).
11. Rowe, T. B., Macrini, T. E. & Luo, Z.-X. Fossil evidence on origin of the mammalian brain. *Science* **332**, 955–957 (2011).
12. Rowe, T. B. & Shepherd, G. M. Role of ortho-retronasal olfaction in mammalian cortical evolution. *J. Comp. Neurol.* **524**, 471–495 (2016).
13. Freeman, W. J. The place of 'codes' in nonlinear neurodynamics. *Prog. Brain Res.* **165**, 447–462 (2007).

14. Heck, D. H. et al. Breathing as a fundamental rhythm of brain function. *Front. Neural Circuits* **10**, 115 (2017).
15. Fontanini, A. & Bower, J. M. Slow-waves in the olfactory system: an olfactory perspective on cortical rhythms. *Trends Neurosci.* **29**, 429–437 (2006).
16. Tort, A., Brankačk, J. & Draguhn, A. Respiration-entrained brain rhythms are global but often overlooked. *Trends Neurosci.* **41**, 186–197 (2018).
17. Biskamp, J., Bartos, M. & Sauer, J.-F. Organization of prefrontal network activity by respiration-related oscillations. *Sci. Rep.* **7**, 45508 (2017).
18. Zhong, W. et al. Selective entrainment of gamma subbands by different slow network oscillations. *Proc. Natl Acad. Sci. USA* **114**, 4519–4524 (2017).
19. Herrero, J. L., Khuvis, S., Yeagle, E., Cerf, M. & Mehta, A. D. Breathing above the brain stem: volitional control and attentional modulation in humans. *J. Neurophysiol.* **119**, 145–159 (2017).
20. Piarulli, A. et al. Ultra-slow mechanical stimulation of olfactory epithelium modulates consciousness by slowing cerebral rhythms in humans. *Sci. Rep.* **8**, 6581 (2018).
21. Cao, Y., Roy, S., Sachdev, R. N. & Heck, D. H. Dynamic correlation between whisking and breathing rhythms in mice. *J. Neurosci.* **32**, 1653–1659 (2012).
22. Moore, J. D. et al. Hierarchy of orofacial rhythms revealed through whisking and breathing. *Nature* **497**, 205–210 (2013).
23. Sirotin, Y. B., Costa, M. E. & Laplagne, D. A. Rodent ultrasonic vocalizations are bound to active sniffing behavior. *Front. Behav. Neurosci.* **8**, 399 (2014).
24. Wong, J. & Waters, D. The synchronisation of signal emission with wingbeat during the approach phase in soprano pipistrelles (*Pipistrellus pygmaeus*). *J. Exp. Biol.* **204**, 575–583 (2001).
25. Suthers, R. A., Thomas, S. P. & Suthers, B. J. Respiration, wing-beat and ultrasonic pulse emission in an echo-locating bat. *J. Exp. Biol.* **56**, 37–48 (1972).
26. Kleinfeld, D., Deschênes, M., Wang, F. & Moore, J. D. More than a rhythm of life: breathing as a binder of orofacial sensation. *Nat. Neurosci.* **17**, 647–651 (2014).
27. Zelano, C. et al. Nasal respiration entrains human limbic oscillations and modulates cognitive function. *J. Neurosci.* **36**, 12448–12467 (2016).
28. Bensafi, M. et al. Olfactomotor activity during imagery mimics that during perception. *Nat. Neurosci.* **6**, 1142–1144 (2003).
29. Arshamian, A., Iravani, B., Majid, A. & Lundström, J. N. Respiration modulates olfactory memory consolidation in humans. *J. Neurosci.* **38**, 10286–10294 (2018).
30. Nakamura, N. H., Fukunaga, M. & Oku, Y. Respiratory modulation of cognitive performance during the retrieval process. *PLoS One* **13**, e0204021 (2018).
31. Frost, R., Siegelman, N., Narkiss, A. & Afek, L. What predicts successful literacy acquisition in a second language? *Psychol. Sci.* **24**, 1243–1252 (2013).
32. Uecker, A. et al. Neuroanatomical correlates of implicit and explicit memory for structurally possible and impossible visual objects. *Learn. Mem.* **4**, 337–355 (1997).
33. Rubinson, M. et al. Hierarchy measurement for modeling network dynamics under directed attacks. *Phys. Rev. E* **96**, 052307 (2017).
34. Barry, R. J., Clarke, A. R. & Johnstone, S. J. A review of electrophysiology in attention-deficit/hyperactivity disorder: I. Qualitative and quantitative electroencephalography. *Clin. Neurophysiol.* **114**, 171–183 (2003).
35. Renault, B., Ragot, R., Lesevre, N. & Remond, A. Onset and offset of brain events as indices of mental chronometry. *Science* **215**, 1413–1415 (1982).
36. Kenemans, J., Kok, A. & Smulders, F. Event-related potentials to conjunctions of spatial frequency and orientation as a function of stimulus parameters and response requirements. *Electroencephalogr. Clin. Neurophysiol.* **88**, 51–63 (1993).
37. Pascual-Marqui, R. D., Michel, C. M. & Lehmann, D. Low resolution electromagnetic tomography: a new method for localizing electrical activity in the brain. *Int. J. Psychophysiol.* **18**, 49–65 (1994).
38. Grech, R. et al. Review on solving the inverse problem in EEG source analysis. *J. Neuroeng. Rehabil.* **5**, 25 (2008).
39. Pascual-Marqui, R. D. Review of methods for solving the EEG inverse problem. *Int. J. Bioelectromagn.* **1**, 75–86 (1999).
40. Brown, R. P. & Gerbarg, P. L. Sudarshan Kriya yogic breathing in the treatment of stress, anxiety, and depression: part I—neurophysiologic model. *J. Altern. Complement. Med.* **11**, 189–201 (2005).
41. Park, H.-J. & Friston, K. Structural and functional brain networks: from connections to cognition. *Science* **342**, 1238411 (2013).
42. Egner, T. & Gruzelier, J. H. EEG biofeedback of low beta band components: frequency-specific effects on variables of attention and event-related brain potentials. *Clin. Neurophysiol.* **115**, 131–139 (2004).
43. Bassett, D. S. & Bullmore, E. Small-world brain networks. *Neuroscientist* **12**, 512–523 (2006).
44. Stam, C. J., Jones, B., Nolte, G., Breakspear, M. & Scheltens, P. Small-world networks and functional connectivity in Alzheimer's disease. *Cereb. Cortex* **17**, 92–99 (2006).
45. Micheloyannis, S. et al. Small-world networks and disturbed functional connectivity in schizophrenia. *Schizophr. Res.* **87**, 60–66 (2006).
46. Naim-Feil, J. et al. Altered brain network dynamics in schizophrenia: a cognitive electroencephalography study. *Biol. Psychiatry Cogn. Neurosci. Neuroimaging* **3**, 88–98 (2018).
47. Klimesch, W., Sauseng, P. & Hanslmayr, S. EEG alpha oscillations: the inhibition–timing hypothesis. *Brain Res. Rev.* **53**, 63–88 (2007).
48. Ritter, P., Moosmann, M. & Villringer, A. Rolandic alpha and beta EEG rhythms' strengths are inversely related to fMRI-BOLD signal in primary somatosensory and motor cortex. *Hum. Brain Mapp.* **30**, 1168–1187 (2009).
49. Janzen, G. & Weststeijn, C. G. Neural representation of object location and route direction: an event-related fMRI study. *Brain Res.* **1165**, 116–125 (2007).
50. Del Negro, C. A., Funk, G. D. & Feldman, J. L. Breathing matters. *Nat. Rev. Neurosci.* **19**, 351–367 (2018).
51. Dlouhy, B. J. et al. Breathing inhibited when seizures spread to the amygdala and upon amygdala stimulation. *J. Neurosci.* **35**, 10281–10289 (2015).
52. Nobis, W. P. et al. Amygdala-stimulation-induced apnea is attention and nasal-breathing dependent. *Ann. Neurol.* **83**, 460–471 (2018).
53. Birn, R. M., Murphy, K., Handwerker, D. A. & Bandettini, P. A. fMRI in the presence of task-correlated breathing variations. *Neuroimage* **47**, 1092–1104 (2009).
54. Simonsohn, U., Nelson, L. D. & Simmons, J. P. p-Curve and effect size: correcting for publication bias using only significant results. *Perspect. Psychol. Sci.* **9**, 666–681 (2014).
55. Kozma, R. & Freeman, W. Analysis of visual theta rhythm—experimental and theoretical evidence of visual sniffing. In *IJCNN'01. International Joint Conference on Neural Networks* 1118–1121 (IEEE, 2001).
56. Faul, F., Erdfelder, E., Lang, A. G. & Buchner, A. G*Power 3: a flexible statistical power analysis program for the social, behavioral, and biomedical sciences. *Behav. Res. Methods* **39**, 175–191 (2007).
57. Johnson, B. N., Russell, C., Khan, R. M. & Sobel, N. A comparison of methods for sniff measurement concurrent with olfactory tasks in humans. *Chem. Senses* **31**, 795–806 (2006).
58. Homan, R. W., Herman, J. & Purdy, P. Cerebral location of international 10–20 system electrode placement. *Electroencephal. Clin. Neurophysiol.* **66**, 376–382 (1987).
59. Gratton, G., Coles, M. G. & Donchin, E. A new method for off-line removal of ocular artifact. *Electroencephal. Clin. Neurophysiol.* **55**, 468–484 (1983).
60. Koenig, T., Kottlow, M., Stein, M. & Melie-García, L. Ragu: a free tool for the analysis of EEG and MEG event-related scalp field data using global randomization statistics. *Comput. Intell. Neurosci.* **2011**, 938925 (2011).
61. Bailey, N. et al. Mindfulness meditators show altered distributions of early and late neural activity markers of attention in a response inhibition task. Preprint at https://www.biorxiv.org/content/10.1101/396259v1 (2018).
62. Xia, M., Wang, J. & He, Y. BrainNet Viewer: a network visualization tool for human brain connectomics. *PLoS One* **8**, e68910 (2013).
63. Tibshirani, R. The lasso method for variable selection in the Cox model. *Stat. Med.* **16**, 385–395 (1997).
64. Antony, A. R. et al. Functional connectivity estimated from intracranial EEG predicts surgical outcome in intractable temporal lobe epilepsy. *PLoS One* **8**, e77916 (2013).

Acknowledgements

This work was supported by grant 1599/14 from the Israel Science Foundation, a grant from Joy Ventures and by the Rob and Cheryl McEwen Fund for Brain Research. The funders had no role in study design, data collection and analysis, decision to publish or preparation of the manuscript.

Author contributions

O.P. and N.S. developed the idea for the study. O.P., A.E., T.S. and N.M. designed and ran the experiments. O.P., A.R. and M.R. analysed the data. O.P., L.S. and N.S. wrote the manuscript.

Competing interests

The authors declare no competing interests.

Additional information

Supplementary information is available for this paper at https://doi.org/10.1038/s41562-019-0556-z.

Reprints and permissions information is available at www.nature.com/reprints.

Correspondence and requests for materials should be addressed to O.P. or N.S.

Publisher's note: Springer Nature remains neutral with regard to jurisdictional claims in published maps and institutional affiliations.

nature research

Corresponding author(s): Noam Sobel and Ofer Perl

Reporting Summary

Nature Research wishes to improve the reproducibility of the work that we publish. This form provides structure for consistency and transparency in reporting. For further information on Nature Research policies, see Authors & Referees and the Editorial Policy Checklist.

Statistical parameters

When statistical analyses are reported, confirm that the following items are present in the relevant location (e.g. figure legend, table legend, main text, or Methods section).

n/a	Confirmed
☐	☒ The exact sample size (*n*) for each experimental group/condition, given as a discrete number and unit of measurement
☐	☒ An indication of whether measurements were taken from distinct samples or whether the same sample was measured repeatedly
☐	☒ The statistical test(s) used AND whether they are one- or two-sided *Only common tests should be described solely by name; describe more complex techniques in the Methods section.*
☐	☒ A description of all covariates tested
☐	☒ A description of any assumptions or corrections, such as tests of normality and adjustment for multiple comparisons
☐	☒ A full description of the statistics including central tendency (e.g. means) or other basic estimates (e.g. regression coefficient) AND variation (e.g. standard deviation) or associated estimates of uncertainty (e.g. confidence intervals)
☐	☒ For null hypothesis testing, the test statistic (e.g. *F*, *t*, *r*) with confidence intervals, effect sizes, degrees of freedom and *P* value noted *Give P values as exact values whenever suitable.*
☒	☐ For Bayesian analysis, information on the choice of priors and Markov chain Monte Carlo settings
☒	☐ For hierarchical and complex designs, identification of the appropriate level for tests and full reporting of outcomes
☐	☒ Estimates of effect sizes (e.g. Cohen's *d*, Pearson's *r*), indicating how they were calculated
☐	☒ Clearly defined error bars *State explicitly what error bars represent (e.g. SD, SE, CI)*

Our web collection on statistics for biologists may be useful.

Software and code

Policy information about availability of computer code

Data collection	Psyscope X B57, Biosemi Actiview 7, LabChart 7.25
Data analysis	MATLAB (multiple versions), Brainvision Analyzer 2.1, RAGU 2017, sLORETA v20170220

For manuscripts utilizing custom algorithms or software that are central to the research but not yet described in published literature, software must be made available to editors/reviewers upon request. We strongly encourage code deposition in a community repository (e.g. GitHub). See the Nature Research guidelines for submitting code & software for further information.

Data

Policy information about availability of data

All manuscripts must include a data availability statement. This statement should provide the following information, where applicable:

- Accession codes, unique identifiers, or web links for publicly available datasets
- A list of figures that have associated raw data
- A description of any restrictions on data availability

All raw data will be available on our lab website upon manuscript publication. This is clearly stated in the manuscript.

Field-specific reporting

Please select the best fit for your research. If you are not sure, read the appropriate sections before making your selection.

☐ Life sciences ☒ Behavioural & social sciences ☐ Ecological, evolutionary & environmental sciences

For a reference copy of the document with all sections, see nature.com/authors/policies/ReportingSummary-flat.pdf

Behavioural & social sciences study design

All studies must disclose on these points even when the disclosure is negative.

Study description	All data in this manuscript are quantitative, based on discrete behavioral responses or acquired continuous signals
Research sample	Research sample in this study comprised of students of the Weizmann Institute of Science and the Hebrew University of Jerusalem (Rehovot campus), ranging in age between 20-36 years (Mean age across all cohorts 25.6 Y.O, 47% Female).
Sampling strategy	We recruited 30 participants per condition, i.e., a cohort similar in size to previous studies of this type (e.g., reference 26). For the internal replication experiment, we conducted Power Analysis using G*Power software (reference 42) which indicated that for power = 0.8 we need to recruit n = 18.
Data collection	Participants' data were collected using signal acquisition software (for physiology and EEG) and input via computer keyboard. Participants were alone in the experimental room during the session. This was a within-subject design, both experimental conditions (e.g., Inhale and Exhale) were present within each session, therefore the experimenters could not affect the results.
Timing	Data were collected over the course of the leading author's PhD studies, between 2013-2018.
Data exclusions	In experiments involving phase-locking of stimulus to respiratory phase, trials that were presented erroneously not locked to inhalation or exhalation onset (confirmed by instantaneous phase value) were discarded prior to analysis (on average, ~10% of trials). The first trial of session was discarded to account for lack of attention or surprise brought about by session start (one out of 160). In ERP-EEG analysis, epochs containing artifacts were discarded using semiautomatic exclusion criteria set to default by the software (3-5% of the epochs). In topographical ANOVA, data underwent multi-dimensional scaling to remove outlier ERP data using Mahalanobis distance, thresholded at $p<0.05$ (default setting of RAGU). This led to the exclusion of 3 participants' data. In the EEG at rest sessions, the dataset of about 600 epochs was randomly down-sampled (random selection of trials) to 200 to reduce computational load.
Non-participation	The expereimental procedure was describecd in detail before participants arrived at the lab. On experiment day no participants refused to participate or dropped out mid-experiment.
Randomization	The experimental designs used were within-participant, therefore no randomization into groups was needed.

Reporting for specific materials, systems and methods

Materials & experimental systems

n/a	Involved in the study
☒	☐ Unique biological materials
☒	☐ Antibodies
☒	☐ Eukaryotic cell lines
☒	☐ Palaeontology
☒	☐ Animals and other organisms
☐	☒ Human research participants

Methods

n/a	Involved in the study
☒	☐ ChIP-seq
☒	☐ Flow cytometry
☒	☐ MRI-based neuroimaging

Human research participants

Policy information about studies involving human research participants

Population characteristics	See above
Recruitment	Participants were recruited via online ads regularily published by our group in specialized "human experimentation" groups in the social media.